Articles

Aldol-Promoted Reaction of R106-Sarcosine: Synthesis and Conformational Analysis of Novel R106 Analogs

Michael J. Rodriguez*,† and Mark J. Zweifel

Infectious Disease Research, Lilly Research Laboratories, Eli Lilly and Company, Indianapolis, Indiana 46285

Richard J. Loncharich*

Computational Chemistry and Molecular Structure Research, Lilly Research Laboratories, Eli Lilly and Company, Indianapolis, Indiana 46285

Received August 10, 1995[⊗]

A unique semisynthetic pathway has been used as a route to novel R106 derivatives. R106-sarcosine, **2**, was discovered to be a key intermediate to obtain these derivatives using classical aldol alkylation conditions. Surprisingly, the site of alkylation on **2** was found to be conformationally hindered which yielded both the D and L isomers of R106-1 (aureobasidin A), **1**, and other new R106 derivatives. The scope of the alkylation was found to be highly dependent upon the reactivity potential of the electrophile. Semiempirical calculations on R106-1 and 8-(*N*-methylthrenonine)-aureobasidin A, **7**, were performed to investigate the thermodynamic stabilities of the D and L isomers. By contrast to stable conformations observed by two X-ray crystal structures of aureobasidins, the calculations indicated that the D isomers were significantly more stable. Furthermore, model semiempirical calculations to probe facial selecitivty were consistent with results obtained experimentally.

Introduction

R106-1 (LY295337), **1**, is part of the R106 family also known as the aureobasidins (Figure 1). Aureobasidins macrocyclic depsipeptides are a new class of promising fungicidal agents produced by fermentation of the microorganism *Aureobasidium pullulans* R106.[1] R106-1 is the major component of fermentation, and since its discovery by Takara Shuzo Pharmaceuticals, several other naturally occurring factors have been isolated and identified.[2] R106-1 is one of the most potent factors that exhibits excellent *in vitro* activity against several clinically important fungal pathogens such as *Candida albicans* and *Cryptococcus neoformans*.[3]

Recent experimental studies[4,5] of R106 aureobasidins provide detailed structural and conformational information that may be useful in addressing how biological activity is manifested by these compounds. These studies of the drug itself only provide pivotal clues into elucidation of structure−activity relationship since specific details of receptor−drug interactions are not known. Our work here complements these studies by providing additional information about the energetics of conformation. We also develop a unique semisynthetic approach to discovery of new R106 derivatives. Further structural analysis of R106 analogs provides a more complete picture of the structural requirements for biological activity of the aureobasidins, but as with the previous studies[4,5] information of specific receptor−drug interactions is still lacking. We first focus on our experimental approach, followed by computational analysis and comparison of two macrocyclic aureobasidins.

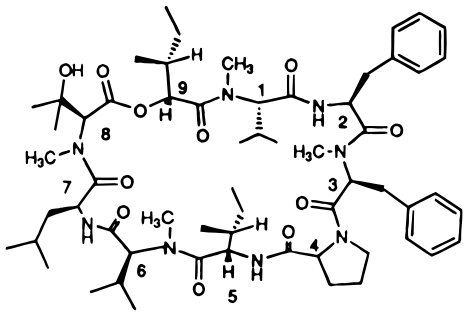

Figure 1. Structure and residue numbering of R106-1 (LY295337).

Results and Discussion

Chemistry. The natural product, **1**, is highly lipophilic and has proven to be a challenge to modify chemically. R106-1 is a cyclic depsipeptide consisting of an octapeptide linked by a (2*R*,3*R*)-2-hydroxy-3-methyl-

† Please send all correspondence to: Dr. Michael J. Rodriguez, Lilly Research Laboratories, Lilly Corporate Center, Indianapolis, IN 46285-1523. Telephone: (317) 276-0305. Telefax: (317) 276-5431. Internet: rodriguez_michael_j@lilly.com.

⊗ Abstract published in *Advance ACS Abstracts,* February 1, 1996.

(1) Yoshikawa, Y.; Ikai, K.; Umeda, Y.; Ogawa, A.; Takesako, K.; Kato, I.; Naganawa, H. *J. Antibiot.* **1993,** *46 (9),* 1347.

(2) Takesako, K.; Ikai, K.; Shimanaka, K.; Yamamoto, J.; Haruna, F.; Nakamura, T.; Yamaguchi, H.; Uchida, K. JP 03044398, 1989.

(3) Takesako, K.; Kuroda, H.; Inoue, T.; Haruna, F.; Yoshikawa, Y.; Kato, I.; Uchida, K.; Hiratani, T.; Yamaguchi, H.. *J. Antibiot.* **1993**, *46 (9),* 1414.

(4) Ohkuma, T.; Hiraga, H.; Igarashi, H. Nippon Kayaku Kabushiki Kaisha, World Patent WO-9400490-A1.

(5) (a) Fujikawa, A.; In, Y.; Inoue, M.; Ishida, T. *J. Org. Chem.* **1994**, *59*, 570. (b) Ishida, T.; In, Y.; Fujikawa, A.; Urata, H.; Inoue, M.; Ikai, K.; Takesako, K.; Kato, I. *J. Chem. Soc., Chem. Commun.* **1992**, *17,* 1231.

0022-3263/96/1961-1564$12.00/0

Scheme 1

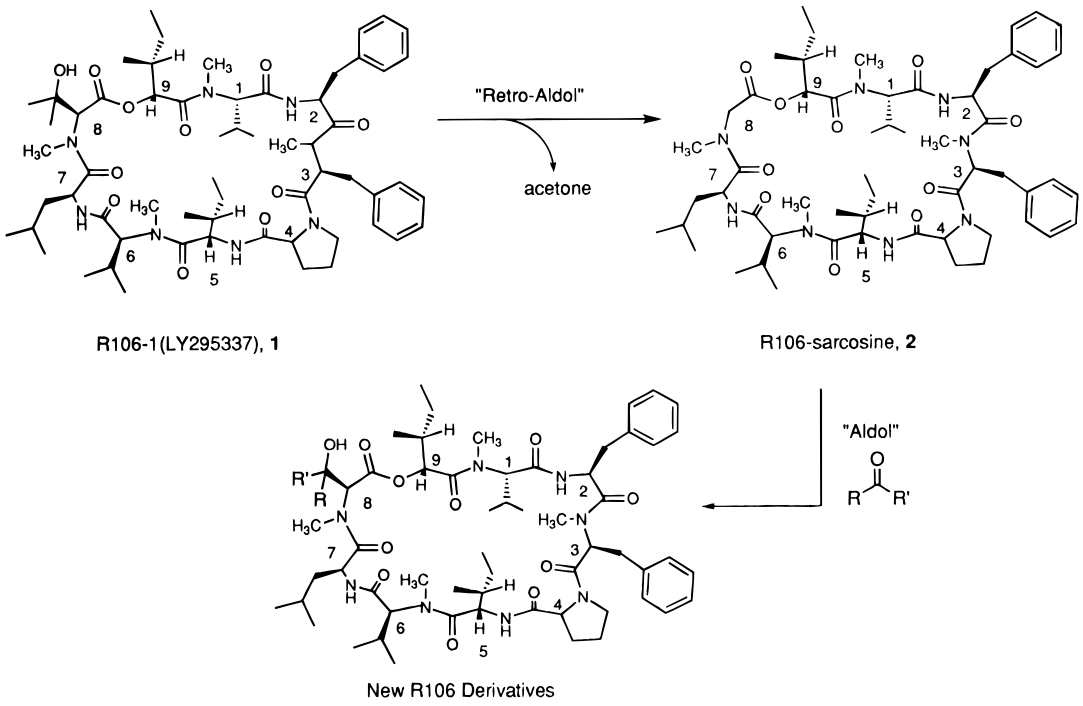

pentanoic acid (Hmp) group at residue 9. The eight peptides have no functionality (chemical handles) available for direct modification with the exception of a hydroxylated *N*-methylvaline residue (HO Me-Val-8). The use of organic and inorganic bases such as sodium hydroxide and triethylamine was reported by Takara Shuzo to obtain R106-sarcosine, **2**, from R106-1 in moderate yields via a retroaldol reaction.[6] Although this R106 derivative was found to be biologically inactive,[7] we recognized that the removal of the tertiary alcohol provided a new chemical handle in the form of a sarcosine residue that would be amenable to classical carbanion chemistry. The utilization of R106-sarcosine as the key intermediate in the aldol-promoted alkylation as shown in Scheme 1 provided direct access to novel R106 derivatives that were otherwise unattainable except via total synthesis.[8]

The conditions developed by Seebach et al. who succesfully alkylated sarcosine residues on linear and cyclic peptides were employed.[9] Other aldol-promoting reagents such as using LiHMDS and alkyl-lithium reagents gave product but in lower yields. Typically, the aldol reaction consisted of dissolving R106-sarcosine in dry THF treated with LiCl. Excess LDA was used to generate a polylithiated species. Subsequent addition of an equal amount of *n*-butyllithium produced an emerald green colored solution, at which point excess electrophile was added and allowed to stir for several hours before quenching with pH 7 buffer.

Since strong basic conditions were used to deprotonate **2**, epimerization of the stereogenic centers was considered to be a potential problem. The extent of epimerization was unknown and to address this issue, **2** was subjected to deprotonation conditions described earlier. The polylithiated species was quenched with acetic acid, and the crude reaction mixture was analyzed by C-18 reversed phase HPLC. No additional products were detected by HPLC. Proton NMR analysis of the purified material was compared and found to be identical to the starting material. The results of the NMR analysis supports that no epimerization of the stereogenic centers takes place under the alkylation conditions.[10]

Determination of Product Ratios. Alkylation of **2** using different ketones and aldehydes are summarized in Tables 1 and 2, respectively. Acetone played a unique role in optimizing the reaction conditions since the aldol products were easily compared and analyzed against the natural product standard, R106-1. By C-18 reversed phase HPLC, a single peak having an identical retention time as the standard was detected. FAB-MS and amino acid analysis of the purified material confirmed that monoalkylation took place at residue 8. We determined the diastereomeric ratios by examining proton NMR signals at 5.75 and 6.49 ppm corresponding to 2-C-*H* Hmp and C_δ(Ar)-*H* MePhe (see residues 9 and 3 in Figure 2), respectively. This proved to be an invaluable method to measure quantitatively the D/L ratios of new compounds derived from ketones. By ^{1}H NMR, the single peak detected by HPLC was a mixture of two products identified as the D and L isomers of R106-1, **3**. As shown

(6) (a) Ikai, K. ; Takesako, K.; Shiomi, K.; Moriguchi, M.; Umeda, Y.; Yamamoto, J.; Kato, I.; Naganawa, H.. *J. Anitbiotics* **1991**, *44 (9)*, 925. (b) Ikai, K.; Shiomi, K.; Takesako, K.; Mizutani, S.; Yamamoto, J.; Ogawa, Y.; Ueno, M.; Kato, I. *J. Anitbiot.* **1991**, *44 (11)*, 1187.

(7) Yamaguchi, H.; Nakamura, T.; Uchida, K.; Takesako, K.; Ikai, K.; Yamamoto, J.; Shimanaka, K. EP 0 443 719, 1991.

(8) Kurome, T.; Inami, K.; Inoue, T.; Ikai, K.; Takesako, K.; Kato, I.; Shiba, T. *Chem. Lett.* **1993**, *11*, 1873.

(9) We found the second equivalent of base as reported by Seebach and co-workers to be important in preventing competition between diisopropylamine and the electrophile. Examples of using Seebach's methodology to alkylate peptides: (a) Seebach, D.; Boes, M.; Naef, R.; Schweizer, W. *J. Am. Chem. Soc.* **1983**, *105 (16)*, 5390. (b) Laube, T.; Dunitz, J.; Seebach, D. *Helv. Chim. Acta* **1985**, *68 (5)*, 1373−93, 1507. (c) Seebach, D.; Bossler, H.; Grundler, H.; Shoda, S. *Helv. Chem. Acta* **1991**, *74*, 197. (d) Miller, S.; Griffiths, S.; Seebach, D. *Helv. Chem. Acta* **1993**, *76*, 563. (e) Seebach, D.; Beck, A.; Bossler, H.; Gerber, C.; Ko, S.; Murtiashaw, C.; Naef, R.; Shoda, S.; Thaler, A. et al. *Helv. Chem. Acta* **1993**, *76*, 1564. (f) Bossler, H.; Seebach, D. *Helv. Chem. Acta* **1994**, *77*, 1124.

(10) (a) These observations were reported by Seebach et al. with peptides containing sacosine units. (ref 9c, p 204). (b) Within the detection limits of ^{1}H NMR, we see no epimerization.

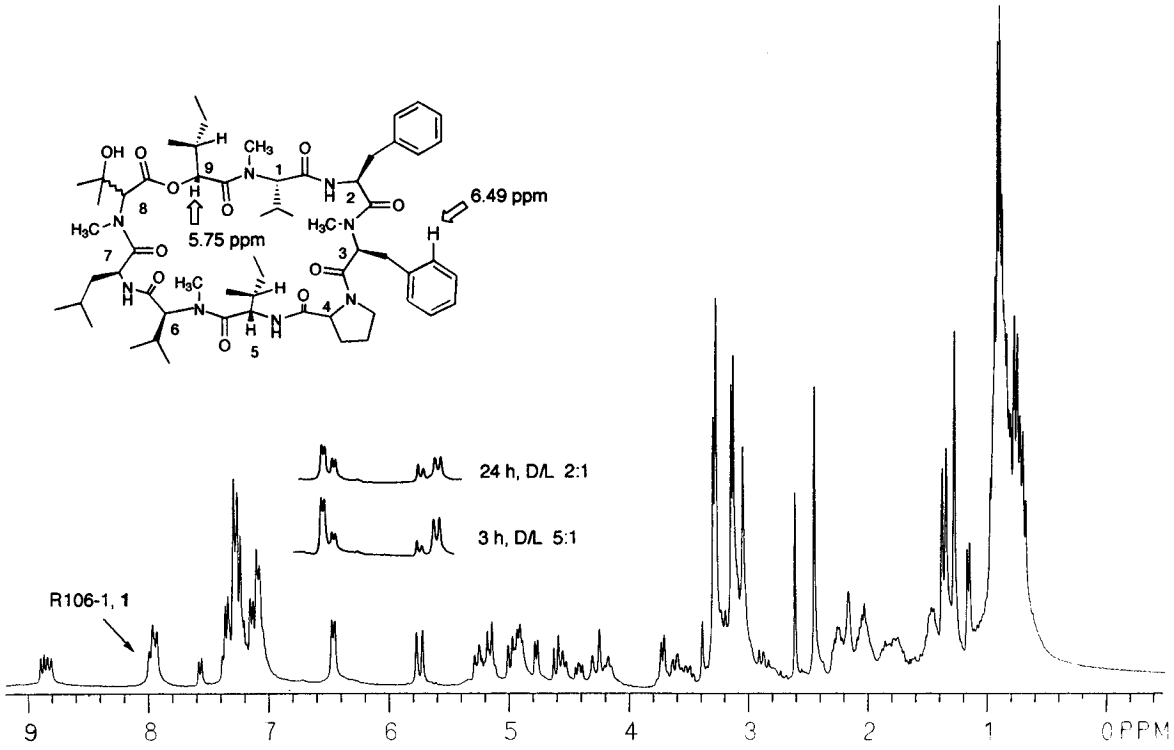

Figure 2. Proton NMR (300 MHz) spectrum of diastereomeric mixture of D and L isomers of R106-1.

Table 1. Alkylation of R106-Sarcosine, 2, with Ketones

electrophile	product	temp (°C)	rxn time (h)	salt (8 equiv)	base (5 equiv/5 equiv)	D/L ratios[a]
acetone	**3**	−78	3	LiCl	LDA/nBuLi	2:1
		−78	24	LiCl	LDA/nBuLi	5:1
		−78	3	LiCl	LDA/nBuLi	3.3:1
		−78 → −45	3	$MgCl_2$	LDA/nBuLi	1:1
			3	LiCl	MeLi/−	3:1
2-butanone[b]	**4**	−78	3	LiCl	LDA/nBuLi	A: 3.6:1 B: 4.0:1
3-pentanone	**5**	−78	2	LiCl	LDA/nBuLi	12:1
cyclopentanone	**6**	−78	3	LiCl	LDA/nBuLi	3.5:1
2-pentanone	no reaction	−78	3	LiCl	LDA/nBuLi	−

[a] D/L ratios of inseparable mixtures of diastereomers were determined by ^{1}H NMR. [b] In this case, two out of the four possible diastereomers were separated by HPLC. D/L ratios of A and B were determined by ^{1}H NMR.

Table 2. Alkylation of R106-Sarcosine, 2, with Aldehydes

						product ratios[a]			
electrophile	product	temp (°C)	rxn time (h)	salt (8 equiv)	base (5 equiv/5 equiv)	A	B	C	D
acetaldehyde	**7**	−78	2	LiCl	LDA/nBuLi	7	12	27	54
		−78	3	−	LDA/nBuLi	4	60	9	27
butyraldehyde	**8**	−78	2	LiCl	LDA/nBuLi	23	15	24	38
		−78	2	−	LDA/nBuLi	12	28	40	20
		−78	2	LiCl	TMP/nBuLi[b]	18	11	25	46
		−78	3	CsCl	LDA/nBuLi	9	27	41	23
		−100	0.5	LiCl	MeLi/−	17	17	43	23
		−78	3	LiCl	LDA/nBuLi	24	15	30	31

[a] HPLC (A → D, in order of elution) product ratios of crude reaction mixtures. Compounds A, D and B, C were assigned the L and D amino acid configuration at residue 8. [b] TMP: Harpoon Base.

in Table 1, by altering the aldol reaction conditions, such as raising the temperature and lengthening the reaction times, higher D/L ratios were obtained (D/L 1:1 to 5:1). Additionally, we observed an increase in the D/L ratio as the size of the electrophile was increased, possibly due to increasing steric hindrance (see Table 1, i.e., acetone → 3-pentanone, **3**−**5**) . If the electrophile was too bulky, as in the case of 2-pentanone, the reaction was sluggish and only starting material was recovered.

Unlike ketones, products derived from aldehydes gave a mixture of four diastereomers (**7**, **8 A**−**D**) that were easily separated by preparative C-18 reversed phase HPLC. As shown in Table 2, we attempted to improve the product ratios by altering reaction conditions but noted only subtle differences in selectivity.

The trend in chemical shifts of the ketone derivatives provided a means in assigning the stereochemistry of the secondary alcohols. We observed that all protons of 2-C-*H* HMP shifted slightly downfield and C_δ(Ar)-*H* MePhe protons shifted slighly upfield for diastereomers having the D configuration. Based on this trend, products

A and **D** were assigned the L configuration and **B** and **C** were assigned the D configuration.

The isolation of products favoring the D configuration indicated an inherent facial selectivity at the site of alkylation is controlling the outcome of the aldol reaction. The preference of D over the L configuration at residue 8 was unexpected since the natural product (R106-1) existed in a stable conformation with the tertiary alcohol in the L configuration. These results prompted us to perform theoretical calculations of the D and L isomers of R106-1 to elucidate the reason for their thermodynamic stabilities as well as to explain the inherent alkylation selectivity.

Thermodynamic Stability of R106-1. We were surprised by the fact that the X-ray crystal structure of R106-1 isolated from the fermentation broth[11] of a strain of *A. pullulans*[1] revealed the natural L configuration of residue 8. A structural analysis of R106 aureobasidins by Ohkuma et al.[4] and by Ishida et al.[5] revealed that the β-hydroxy group of residue 8 (HO Me-Val-8) is hydrogen-bonded in a bifurcated fashion to two carbonyl oxygens, namely, Leu-7 (2.010 Å) and Me-Val-8 (2.867 Å).[4] This hydrogen-bonded network is the underpinning that stabilizes the γ-turn conformation[4,5] and is further hypothesized as necessary for binding with the receptor[5] and possibly required for manifestation of activity.[5]

In order to understand more about the relative stabilities of the six possible isomers of R106-1, relevent to residue 8, we performed semiempirical optimization of each structure. We chose the AM1 semiempirical method because it was originally developed to study molecules of biological interest and to better reproduce inherent hydrogen bonding features[12] in these systems, which are critical to the aureobasidins. We further probed the inherent stabilization via internal hydrogen bonding in several of the isomers by carrying out constrained optimizations. The six isomers optimized by the AM1 method[13] are shown in Figure 3, and the absolute and relative values of the heats of formation are presented in the Table 3. The computational results overwhelmingly indicate that the D isomer is thermodynamically more stable than the L isomer. A Boltzmann distribution at −78 °C of the AM1 heats of formation was determined on the six isomers of R106-1. This computation predicts a 99.6:0.4 ratio of D:L isomers. These calculations, however, do not address the selectivity observed in our alkylation experiments, but are consistent with the observed major product.

To elucidate the nature of the thermodynamic stabilities of the isomers of R106-1 we performed some constrained optimizations. For example, AM1 geometry optimization of isomer **1-L-a** was carried out with only the CA-CB-OG-HG dihedral angle of residue 8 constrained to 180°. The final heat of formation of this structure was −416.8 kcal/mol. Comparison of this value with the heat of formation of the fully optimized X-ray structure indicates a −6.5 kcal/mol stabilization due to the bifurcated hydrogen bonds. This value is larger than experimentally obtained −0.5 to −2 kcal/mol enthalpies of stabilization for a variety of hydrogen bond interactions.[14] However, it is more consistent with the −4 to −5 kcal/mol enthalpy of stabilization of 2-propanol dimer.[15] The substantial interaction of the bifurcated hydrogen bonds in the AM1 optimized geometry of isomer **1-L-a** is evidenced by the short hydrogen bonding distances of 2.270 Å [OH···O=C β OH Me-Val-8] and 2.271 Å [OH···O=C Leu-7].

We also performed partial optimization of the L isomer **1-L-c** with only the CA-CB-OG-HG dihedral angle of residue 8 constrained to 180°. The AM1 final heat of formation for this structure was −419.8 kcal/mol. Comparison of the energetics of this structure with that of isomer **1-L-c** (Figure 3) indicates a −4.0 kcal/mol stabilization due to the OH···O=C [β OH Me-Val-8] hydrogen bond at a distance of 2.151 Å. As expected, the stabilization of this lone internal hydrogen bond is less than that of the bifurcated hydrogen-bonded system.

Estimates for the degree of internal hydrogen bonding of the D isomers **1-D-b** and **1-D-c** (Figure 3) were also made by similar constrained optimization. Here, hydrogen bonding stabilizes isomer **1-D-c** by −1.6 kcal/mol via interaction of the OH···O(CO) [β OH Me-Val-8] at a distance of 2.213 Å. Isomer **1-D-c** possesses a hydrogen bond of the hydroxyl group and the carbonyl oxygen of residue 8 with a stabilization of −3.2 kcal/mol.

Although comparison of the degree of internal hydrogen bonding indicates that the X-ray structure conformation **1-L-a** is most stabilized via hydrogen bonding of the 2-propanol side chain this does not explain the energetic preference for the D isomer that we observe in our experiments. Further inspection of the two most perferred L isomers **1-L-a** and **1-L-c** and the preferred D isomer **1-D-b** indicates an additional factor contributes to the D isomer stabilization. The presence of the internal bifurcated hydrogen bond in isomer **1-L-a** causes large O−O repulsions by placing the carbonyl of Leu-7 2.877 Å from the carbonyl of Me-Val-8 and 3.337 Å from the ether oxygen of Hmp-9. Likewise the corresponding distances in isomer **1-L-c** are 3.141 and 3.030 Å. By contrast, the corresponding distances in isomer **1-D-b** are much larger at values of 3.887 and 4.422 Å, which substantially reduces these interactions. To roughly estimate some of the O−O replusion in isomers **1-L-a**, **1-L-c**, and **1-D-b**, we calculated the interaction energies of formic acid and formaldehyde whereby the non-hydrogen atoms of these two species were fixed to the corresponding peptide geometries for the carbonyl of Leu-7 and the ester linkage of Me-Val-8 and Hmp-9. The interaction energy calculations indicate a 4.0, 3.3 and 1.8 kcal/mol destabilization due to the O−O repulsions in isomers **1-L-a**, **1-L-c**, and **1-D-b**, respectively. The L isomers clearly possess much larger destabilizing interactions than the D isomers. Thus the O−O repulsion accounts for a major portion of the thermodynamic stability for the D and L isomers. The additional destabilization of the L isomers relative to the D isomers can be accounted for by the nature of the substitutents about the ϕ angle ($C_7-N_8-CA_8-C_8$). This dihedral angle is 46.1, 37.3, and 92.9° in isomers **1-L-a**, **1-L-c**, and **1-D-b**, respectively. The smaller angle in the L isomers causes greater steric repulsions that are not present in the D isomers. For example, the *N*-methyl group of residue-8

(11) Takesako, K.; Ikai, K.; Haruna, F.; Endo, M.; Shimanaka, K.; Sono, E.; Nakamura, T.; Kato, I; Yamaguchi, H. *J. Antibiot.* **1991**, *44*, 919.

(12) Stewart, J. J. P. In *Reviews in Computational Chemistry*; Lipkowitz, K. B.; Boyd, D. B., Eds; VCH Publishers: New York, 1990; Vol 1, p 45.

(13) Dewar, M. J. S.; Zoebisch, E. G.; Healy, E. F.; Stewart, J. J. P. *J. Am. Chem. Soc.* **1985**, *107*, 3902.

(14) (a) Williams, D. *Aldrichim. Acta* **1991**, *24*, 71. (b) Searle, M. S.; Williams, D. H.; Gerhard, U. *J. Am. Chem. Soc.* **1992**, *114*, 10697.

(15) Curtiss, L. A.; Blander, M. *Chem. Rev.* **1988**, *88*, 827.

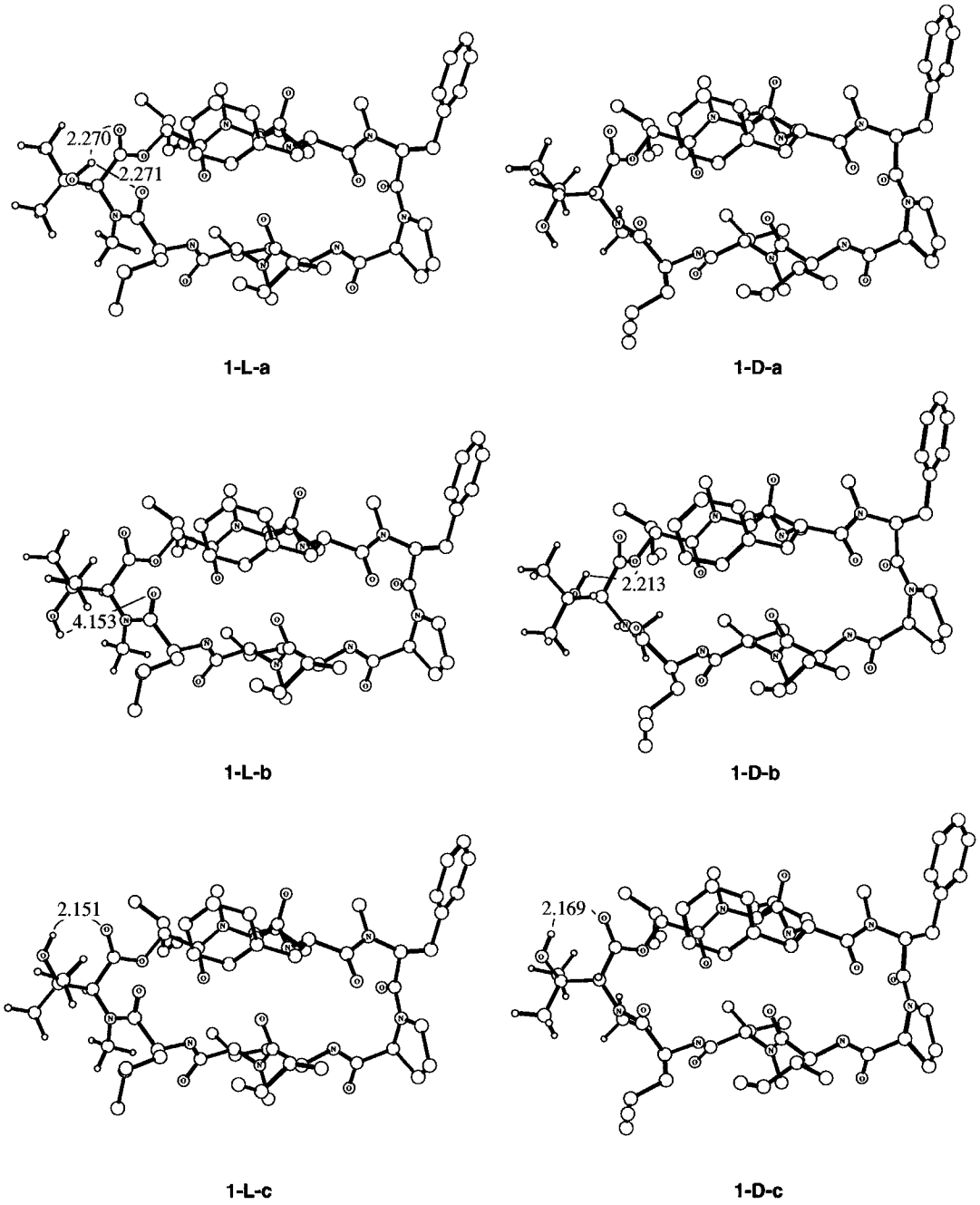

Figure 3. Six AM1 optimized conformers of R106-1. All oxygen and nitrogen atoms are labeled. Additionally, large spheres represent carbon atoms and small spheres represent hydrogen atoms. For clarity only the hydrogen atoms on residue 8 are explicitly shown. Hydrogen bond distances are in angstroms.

Table 3. Absolute and Relative Heats of Formation (kcal/mol) from AM1 Calculations of the Six Isomers of R106-1, 1

isomer	configuration	N−CA−CB−OG	H_f	ΔH_f	H_f[a]	ΔH_f[a]
1-L-a	L	60.2	−423.3	2.7	−423.5	2.6
1-L-b	L	−59.8	−422.1	3.9	−422.4	3.8
1-L-c	L	−175.7	−423.8	2.2	−424.1	2.1
1-D-a	D	50.9	−423.4	2.6	−423.6	2.5
1-D-b	D	−69.7	−426.0	0.0	−426.2	0.0
1-D-c	D	158.9	−424.6	1.4	−424.8	1.3

[a] Calculations use a molecular mechanics correction to insure planarity of amide linkages.

is 2.068 Å from the proton HA, and a side chain methyl group is 2.279 Å from the residue-8 carbonyl oxygen in isomer **1-L-a** (see Figure 3). Likewise in isomer **1-L-c**, the *N*-methyl group HA hydrogen distance is 2.076 Å, while a side chain methyl group is positioned 2.272 Å from the methine proton of Leu-7. Here we did not investigate the specific contribution of these steric interactions caused by the smaller ϕ angle in the L isomers because it is difficult to separate this contribution to destabilization from that of the O−O repulsion. However, noticeable differences in geometry of the γ-turn conformation in the D and L isomers suggest that for better interaction with receptor and increased biological activity the two carbonyls of Leu-7 and Me-Val-8 should be approximately 3 Å apart as demonstrated by isomers **1-L-a** and **1-L-c**.

Alkylation Selectivity of R106-1. In order to understand the origins of alkylation selectivity, we sought a relatively simple and accurate three-dimensional model of the respective transition state for these reactions as described in the Experimental Section. Comparison of

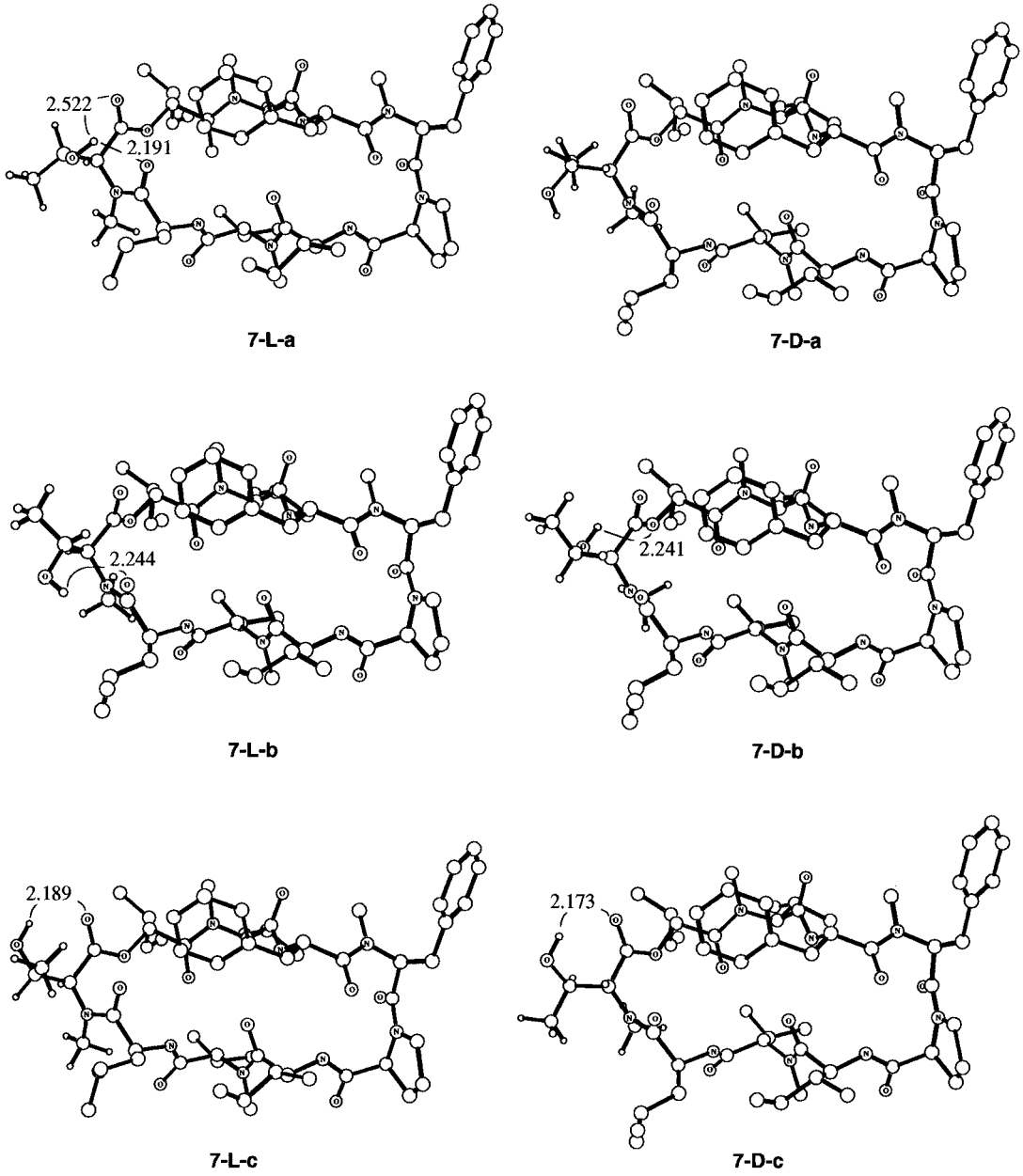

Figure 4. Six AM1 optimized conformers of **7.** For details see Figure 3.

the heats of formation for the alkylation selectivity models give relative energies of 1.5, 2.9, 0.7, 1.6, 0.0, and 1.3 kcal/mol, respectively, for structures leading to isomers **1-L-a**, **1-L-b**, **1-L-c**, **1-D-a**, **1-D-b**, and **1-D-c**. A Boltzmann distribution at −78 °C of the AM1 heats of formation for the six alkylation models predicts an 84:16 ratio of D:L isomers. This result is in accord with experimental observations (Table 1) and suggests that the factors controlling the isomeric stabilities play an important role in determining the selectivity of reaction.

Thermodynamic Stability of 7. We also theoretically investigated the relative stabilities of six isomers of 8-(*N*-methylthrenonine)aureobasidin A, **7**. The optimized structures of the six isomers are shown in Figure 4, and the heats of formation are given in Table 4. As in the case of the tertiary alcohol (residue 8) R106-1, for **7** the calculations again indicate the D isomer is significantly more stable than the L isomer. Moreover, the results of the secondary alcohol are quite similar with that of tertiary alcohol, the D:L ratio as determined by a Boltzmann distribution is 99.25:0.75. Even the destabilization of the isomers relative to the perferred structure compares well with results of the prototype aureobasidin, R106-1, with the exception of isomer **7-L-b**. Comparison of isomer **7-L-b** and **1-L-b** illustrates this completely unexpected finding. That is, as seen in Figure 3, for **1-L-b** there is no hydrogen bonding of the tertiary hydroxylated residue. The distance between the hydroxyl hydrogen and carbonyl oxygen of Leu-7 is 4.153 Å. The steric bulk of the two methyl groups prevent formation of a hydrogen bond. By contrast, in the case of the

Table 4. Absolute and Relative Heats of Formation (kcal/mol) from AM1 Calculations of the Six Isomers of 7

isomer	configuration	N−CA−CB−OG	H_f	ΔH_f	H_f[a]	ΔH_f[a]
7-L-a	L	48.7	−422.5	2.7	−422.7	2.6
7-L-b	L	−41.2	−423.1	2.1	−423.3	2.0
7-L-c	L	−169.8	−422.7	2.4	−422.9	2.3
7-D-a	D	58.1	−422.9	2.2	−423.2	2.1
7-D-b	D	−72.4	−425.1	0.0	−425.3	0.0
7-D-c	D	159.4	−423.0	2.2	−423.2	2.1

[a] Calculations use a molecular mechanics correction to insure planarity of amide linkages.

secondary hydroxylated derivative **7**, a hydrogen bond of the hydroxyl group to the carbonyl oxygen of Leu-7 is well formed. Furthermore, stabilization of this hydrogen bond leads to an energetic perference of this isomer over the other two L isomers. It should be noted that tertiary hydroxylated derivatives, as with R106-1, are active against the fungal pathogen *C. neoformans*, but lose activity as steric bulk of this residue is increased.[16] However, all secondary alcohols are inactive against this fungal pathogen despite seemingly less steric bulk of the residue 8 side chain. More dramatically, with isomer **1-L-b** of R106-1 the hydroxyl group is available to interact with the receptor. However, in all three isomers of the secondary alcohol of the hydroxyl group is tied up via strong internal hydrogen bonding with the macrocyclic backbone and not available for drug-receptor interaction. This suggests a possible structural requirement of residue 8 for manifestation of activity against *C. neoformans*.

We also performed constrained optimization of the isomers of 8-(*N*-methylthreonine)aureobasidin A to determine the strength of internal hydrogen bonding in these structures. The inherent stabilization due to hydrogen bonding involving residue 8 for isomers **7-L-a**, **7-L-b**, **7-L-c**, **7-D-b**, and **7-D-c** is −5.9, −3.1, −5.1, −3.0, and −1.7 kcal/mol, respectively. The results here are similar to corresponding results for R106-1.

Alkylation Selectivity of 7. We also investigated the alkylation selectivity of **7** using our simple model for facial selectivity. Comparison of the heats of formation for the alkylation selectivity models give relative energies of 2.3, 0.8, 1.1, 2.1, 0.0, and 3.2 kcal/mol, respectively, for model structures leading to isomers **7-L-a**, **7-L-b**, **7-L-c**, **7-D-a**, **7-D-b**, and **7-D-c**. The simple alkylation model predicts a larger preference than the experimentally observed product ratio of 69:31 for the D:L isomeric ratio. These calculations are in accord with the preferred thermodynamic product which is the D isomer when the reaction time is 3 h.

Conclusion

The aldol-promoted alkylation of R106-sarcosine provided an opportunity to synthesize and evaluate novel tertiary and secondary hydroxylated R106 derivatives. The scope of the aldol reaction was dependent upon the size of the electrophile used for the alkylation. An increase in the D/L ratio was observed as the size of the electrophile was increased. Calculations of the D and L isomers of **1** and **7** indicated that the D isomers are thermodynamically more stable than the L isomers, although R106 exists in a stable L configuration in the crystalline state.[4,5] Additionally, factors that control the thermodynamic stability are believed to influence the alkylation selectivity. Furthermore, computational analysis of several isomers of **1** and **7** revealed some interesting differences. Due to steric bulk of the two methyl groups of residue 8 in R106-1, the hydrogen bonding between the hydroxyl group and the carbonyl oxygen of leucine-7 is absent in one L conformer. That is, the hydroxyl group can exist in a stable conformation where it is positioned away from the carbonyl and available for receptor interaction. This hydroxyl group interaction would enhance affinity for a target receptor. By contrast, L diastereomers derived from aldehydes as in the case of **7** exist in stable conformations in which the hydroxyl group is hydrogen bonded and unavailable for possible receptor interaction. In addition, comparisons of the calculated geometries of the D and L isomers suggest a 3 Å separation of the Leu-7 and Me-Val-8 carbonyls for biological activity.

Furthermore, the scope of our synthetic experiments to probe structural requirements of residue 8 indicate that only a small steric geometry is tolerated at this position. Although the acetaldehyde derivative, **7**, seems to fit the steric requirements of a target receptor it differs from **1** by the nature of the hydroxyl group as described above. Although, no crystal structure of an aureobasidin-receptor complex has been reported to date, it will be interesting to see if the specific interactions described here will bear resemblance to those eventually found.

Experimental Section

General. ^{1}H NMR spectra were determined at 500 or 300 MHz. Chemical shifts are reported in parts per million (δ) relative to trimethylsiliane as internal standard. Spin multiplicities are reported using the following abbreviations: singlet (s), doublet (d), triplet (t), quartet (q), multiplet (m), and broad (br). Infared spectra were recorded on a Nicolet 510P FT-IR spectrometer. FAB mass spectra were obtained using a V6 ZAB-2SE mass spectrometer. High-resolution masss spectra were generated for all final products and were consistent with the theoretical empirical formulas. Analytical reversed-phase HPLC work was done using the Waters 600E system with Waters Nova-Pak (C18, 3.9 × 300 mm) column (30/70 water/acetonitrile isocratic solvent system) with a flow rate of 1.5 mL/min and using UV detection 250 nm. Preparative HPLC work performed with a Waters Prep 2000 system using Waters 3X preppak Nova-Pak (C18, 40 × 100) column. All final products were >90% pure as determined by analytical HPLC and by ^{1}H NMR. All electrophiles were commercially available and were used without further purification.

D/L Aureobasidin A (3). To a −78 °C solution of R106-sarcosine (100 mg, 0.096 mmol) in dry THF (2.0 mL), treated with LiCl (0.032 mg, 0.77 mmol), was added 0.35 M LDA (1.37 mL) dropwise over a 5 min period. The reaction was allowed to stir for an additional 2 h before the addition of 1.6 M *n*-butyllithium (0.30 mL). After 10 min of stirring, dry acetone (0.11 mL, 1.5 mmol) was added dropwise and the reaction was allowed to stir for additional 3 h before quenching with pH 7 buffer. After warming to room temperature, cold 10% HCl was added to the reaction mixture, and the solution was extracted with EtOAc. The organic phase was washed with water, $NaHCO_3$, and brine, dried over Na_2SO_4, and concentrated. The residue was purified by C-18 reversed phase chromatography (25:75 water/acetonitrile, Waters 3x 40 × 10 Nova-Pak radial cartridges, 75 mL/min, 250 nm). The first eluate was unreacted starting material, R106-sarcosine (24 mg). The second eluate gave the desired product **3**, a 2:1 D/L mixture of R106-1(20 mg, 19%) as a white solid. Analytical HPLC retention time, 11.59 min; IR (KBr) ν 3308, 2967, 2935, 2878, 1733, 1648, 1632 cm^{-1}; ^{1}H NMR (500 MHz) δ 1.18 (d, J = 7.35 Hz), 1.20 (d, J = 7.35 Hz), 1.25 (s), 1.30 (s), 1.32 (s), 1.37 (s), 1.39 (s), 1.42−1.52 (br m), 1.53 (s), 1.62 (s), 1.64−1.85 (m), 1.9 (m), 2.0−2.15 (m), 2.30 (m), 2.46 (s), 2.48 (s), 2.50 (s), 2.60 (s), 2.62 (s), 2.65 (m), 2.90 (s), 2.95 (m), 3.03 (s), 3.05 (m), 3.07 (s), 3.10 (m), 3.14 (s), 3.16 (s), 3.18 (s), 3.27 (m), 3.29 (s), 3.31 (s), 3.3 (s), 3.5 (s), 3.41 (s), 3.55 (m), 3.65 (m), 3.75 (d, J = 8.08 Hz), 3.80 (d, J = 8.08 Hz), 4.23 (m), 4.5 (m), 4.57 (m), 4.62 (d, J = 11.02 Hz), 4.77 (d, J = 7.35 Hz), 4.8 (d, J = 7.35 Hz), 4.08−5.0 (m), 5.03 (d, J = 11.02 Hz), 5.15−5.35 (m), 5.4 (s), 5.44 (m), 5.63 (d, J = 0.73 Hz), 5.69 (d, J = 0.73 Hz), 5.8 (d, J = 0.73 Hz), 6.5 (d, J = 7.35 Hz), 6.58 (d, J = 7.35 Hz), 6.92 (m), 7.05−7.35 (m), 7.4 (d, J = 7.35 Hz), 7.85 (d, J = 8.08 Hz), 7.93 (d, J = 7.35 Hz), 7.95 (d, J = 7.35 Hz), 8.0 (d, J = 7.35 Hz), 8.75 (d, J = 7.35 Hz), 8.83 (d, J = 7.35 Hz), 8.85 (d, J = 7.35 Hz); exact mass calcd for $C_{60}H_{93}N_8O_{11}$ 1101.6964, found 1101.6970.

(16) Rodriguez, M. J.; Zweifel, M. J.; Farmer, J. D.; Gordee, R. S.; Loncharich, R. J. *J. Antibiot.*, in press.

8-(3-Hydroxy-*N*,3-dimethylnorvaline)aureobasidin A (4). According to a procedure similar to that described for **3**, to R106-sarcosine (0.2 g, 0.19 mmol), and LiCl (64 mg, 1.5 mmol) in dry THF (2 mL) was added 0.35 M LDA (2.74 mL) followed by 1.6 M *n*-butyllithium (0.6 mL) and 2-butanone (0.27 mL, 3.1 mmol). The residue was purified by C-18 reversed phase chromatography (30:70 water/acetonitrile, Waters 3x 40 × 10 Nova-Pak radial cartridges, 75 mL/min, 250 nm). The first eluate gave **4A** (22.8 mg, 10.7%): Analytical HPLC retention time, 17.74 min; IR (KBr) ν cm^{-1}; ^{1}H NMR (500 MHz) δ 0.65−1.05 (m), 1.10 (m), 1.18 (d, J = 7.35 Hz), 1.25 (s), 1.35 (s), 1.38 (s), 1.39−1.63 (m), 1.65−2.15 (m), 2.22 (br s), 2.30 (m), 2.48 (s), 2.50 (s), 2.60 (s), 2.94 (d, J = 13.2 Hz), 2.97 (d, J = 13.2 Hz), 3.02 (s), 3.10 (m), 3.12 (s), 3.18 (s), 3.28 (s), 3.30 (s), 3.33 (d, J = 7.35 Hz), 3.55 (m), 3.65 (dd, 14.7, 2.94 Hz), 3.75 (m), 3.80 (d, 8.08 Hz), 4.2 (br t, J = 8.08, 8.08 Hz), 4.5 (d, J = 11.02 Hz), 4.78 (d, J = 7.35 Hz), 4.9 (m), 4.95 (d, J = 11.02 Hz), 5.2 (m), 5.3 (m), 5.4 (d, J = 11.02 Hz), 5.5 (br s), 5.55 (br s), 5.62 (br s), 5.67 (br s), 5.79 (br s), 6.5 (d, J = 7.35 Hz), 6.62 (d, J = 7.35 Hz), 6.93 (d, J = 7.35 Hz), 7.05−7.35 (m), 7.85 (d, J = 8.82 Hz), 7.95 (d, J = 7.35 Hz), 8.77 (d, J = 8.82 Hz), 8.85 (d, J = 8.82 Hz), 8.91 (d, J = 7.35 Hz); exact mass calcd for $C_{61}H_{95}N_8O_{11}$ 1115.7120, found 1115.7154. The second eluate gave **4B** (26.4 mg, 12.4%): Analytical HPLC retention time, 18.80 min; IR (KBr) ν cm^{-1}; ^{1}H NMR (500 MHz) δ 0.65−1.05 (m), 1.10 (m), 1.18 (d, J = 7.35 Hz), 1.23 (s), 1.25 (s), 1.26−1.52 (m), 1.55 (s), 1.57 (m), 1.59 (s), 1.65 (m), 1.75 (m), 1.85 (s), 1.9 (m), 2.0−2.13 (m), 2.30 (m), 2.45 (s), 2.50 (s), 2.63 (s), 2.95 (s), 2.97 (s), 3.03 (s), 3.07 (s), 3.10 (m), 3.13 (s), 3.18 (s), 3.28 (s), 3.30 (s), 3.31 (m), 3.33 (s), 3.35 (s), 3.55 (m), 3.64 (dd, J = 14.7, 2.94 Hz), 3.75 (m), 4.2 (t, J = 8.08, 8.08 Hz), 4.48 (m), 4.52 (d, J = 11.02 Hz), 4.78 (d, J = 7.35 Hz), 4.9 (m), 4.95 (d, J = 11.05 Hz), 5.2 (m), 5.28 (m), 5.32 (d, J = 11.02 Hz), 5.35 (s), 5.4 (s), 5.65 (br s), 5.70 (br s), 5.80 (br s), 6.45 (d, J = 7.35 Hz), 6.57 (d, J = 7.35 Hz), 6.97 (d, J =7.35 Hz), 7.05−7.35 Hz), 7.4 (d, J = 7.35 Hz), 7.87 (d, J = 8.82 Hz), 7.92 (d, J = 7.35 Hz), 8.0 (d, J = 7.35 Hz), 8.80 (d, J = 7.35 Hz), 8.85 (d, J = 8.82 Hz), 8.90 (d, J = 7.35 Hz); exact mass calcd for $C_{61}H_{95}N_8O_{11}$ 1115.7120, found 1115.7133.

8-(3-Ethyl-3-hydroxy-*N*-methylnorvaline)aureobasidin A (5). According to a procedure similar to that described for **3** to R106-sarcosine (0.2 g, 0.19 mmol) and LiCl (64 mg, 1.5 mmol) in dry THF (2 mL) was added 0.35 M LDA (2.75 mL) followed by 1.6 M *n*-butyllithium (0.6 mL) and 3-pentanone (0.32 mL, 3.0 mmol). The residue purified by C-18 reversed phase chromatography (20:80 water/acetonitrile, Waters 3x 40 × 10 Nova-Pak radial cartridges, 75 mL/min, 250 nm) gave **5** (10.5 mg, 5%): Analytical HPLC retention time, 24.44 min; IR (KBr) ν 3323, 2965, 2877, 1739, 1633 cm^{-1}; ^{1}H NMR (500 MHz) δ 0.70−1.15 (m), 1.18 (d, J = 7.35 Hz), 1.25 (s), 1.35−1.65 (m), 1.70 (m), 1.77 (m), 1.82 (br s), 1.84−2.10 (m), 2.30 (m), 2.50 (s), 2.64 (s), 2.67 (m), 2.65 (m), 2.95 (d, J = 13.2 Hz), 2.97 (d, J = 13.2 Hz), 3.05 (s), 3.07−3.18 (m), 3.12 (s), 3.15 (m), 3.17 (s), 3.25 (s), 3.27 (s), 3.29 (s), 3.37 (s), 3.39 (s), 3.55 (m), 3.65 (dd, J = 14.7, 2.94 Hz), 3.75 (m), 3.80 (d, J = 8.82 Hz), 4.23 (t, J = 8.08, 8.08 Hz), 4.5 (m), 4.52 (d, J = 11.02 Hz), 4.78 (d, J = 7.35 Hz), 4.9 (m), 4.95 (d, J = 11.02 Hz), 5.2 (m), 5.28 (m), 5.33 (d, J = 11.02 Hz), 5.45 (s), 5.5 (s), 5.65 (br d, J = 0.73 Hz), 5.68 (br d, J = 0.73 Hz), 5.80 (br s), 6.5 (d, J = 7.35), 6.55 (d, J = 7.35 Hz), 6.97 (d, J = 7.35 Hz), 7.05−7.35 (m), 7.88 (d, J = 8.82 Hz), 7.95 (d, J = 7.35 Hz), 8.0 (d, J = 7.35 Hz), 8.8 (d, J = 8.82 Hz), 8.85 (d, J = 8.82 Hz), 8.9 (d, J = 7.35 Hz); exact mass calcd for $C_{62}H_{97}N_8O_{11}$ 1129.7277, found 1115.7303.

8-[2-(1-Hydroxycyclopentyl)-*N*-methylnorvaline]aureobasidin A (6). According to a procedure similar to that described for **3**, to R106-sarcosine (0.2 g, 0.19 mmol) and LiCl (64 mg, 1.5 mmol) in dry THF (2 mL) was added 0.35 M LDA (2.74 mL) followed by 1.6 M *n*-butyllithium (0.6 mL) and cyclopentanone (0.27 mL, 3.0 mmol). The residue purified by C-18 reversed phase chromatography (30:70 water/acetonitrile, Waters 3x 40 × 10 Nova-Pak radial cartridges, 75 mL/min, 250 nm) gave **6** (24.7 mg, 11.1%): Analytical HPLC retention time, 18.08 min; IR (KBr) ν 3326, 2964, 2876, 1741, 1633 cm^{-1}; ^{1}H NMR (500 MHz) δ 0.65−1.12 (m), 1.18 (br d, J = 7.35 Hz), 1.21 (m), 1.25 (s), 1.27−1.95 (m), 2.0−2.20 (m), 2.25−2.33 (m), 2.48 (s), 2.50 (s), 2.57 (s), 2.63 (d, J = 2.63 Hz), 2.65 (s), 2.67 (m), 2.70 (s), 2.75 (s), 2.78 (s), 2.83 (m), 2.9 (s), 2.93 (s), 2.95 (s), 2.98 (br s), 3.0−3.11 (m), 3.12 (s), 3.15 (s), 3.17 (s), 3.20 (s), 3.28 (s), 3.30 (s), 3.32 (s), 3.34 (s), 3.55 (m), 3.65 (m), 3.72 (m), 3.80 (d, J = 8.08 Hz), 4.22 (m), 4.47 (d, J = 11.02 Hz), 4.5 (m), 4.78 (d, J = 7.35 Hz), 4.9−5.05 (m), 5.17 (m), 5.23 (d, J = 11.02 Hz), 5.3 (m), 5.35 (s), 5.38 (s), 5.4 (s), 5.65 (br s), 5.70 (br s), 5.75 (s), 5.8 (s), 6.5 (d, J = 7.35 Hz), 6.6 (d, J = 7.35 Hz), 7.0−7.35 (m), 7.87 (d, J = 7.87 Hz), 7.93 (d, J = 7.35 Hz), 7.95 (m), 8.78 (d, J = 7.35 Hz), 8.88 (m), 8.9 (d, J = 7.35 Hz); exact mass calcd for $C_{62}H_{97}N_8O_{11}$ 1127.7141, found 1127.7120.

8-(*N*-methylthreonine)aureobasidin A (7). According to a procedure similar to that described for **3**, to R106-sarcosine (0.5 g, 0.48 mmol), and LiCl (160 mg, 3.8 mmol) in dry THF (10 mL) was added 0.3 M LDA (6.6 mL) followed by 1.6 M *n*-butyllithium (1.25 mL) and acetaldehyde (0.12 mL, 2.2 mmol). The residue was purified by C-18 reversed phase chromatography (38:62 water/acetonitrile, Waters 3x 40 × 10 Nova-Pak radial cartridges, 85 mL/min, 250 nm). The first eluate gave **7A** (56.6 mg, 10.9%): Analytical HPLC retention time, 9.35 min; IR (KBr) ν 3322, 2964, 2876, 1750, 1637 cm^{-1}; ^{1}H NMR (500 MHz) δ 0.60−1.12 (m), 1.15 (d, J = 7.35 Hz), 1.23 (m), 1.27 (s), 1.30 (s), 1.37 (m), 1.50 (m), 1.6 (m), 1.65 (m), 1.73 (m), 1.78 (m), 1.88 (m), 1.95−2.10 (m), 2.18 (br s), 2.28 (m), 2.45 (s), 2.55 (s), 2.68 (s), 2.73 (s), 2.83 (s), 2.88 (d, J = 5.88 Hz), 2.93 (d, J = 5.88 Hz), 3.02 (br s), 3.07 (m), 3.18 (s), 3.20 (m), 3.27 (s), 3.32 (s), 3.4 (br d, 3.67 Hz), 3.53 (m), 3.57 (m), 3.60−3.70 (m), 3.73 (d, J = 8.08 Hz), 3.9 (br s), 4.2 (br t, 7.35, 7.35 Hz), 4.45 (m), 4.52 (m), 4.58 (d, J = 11.02 Hz), 4.78 (d, J = 7.35 Hz), 4.9 (dd, J = 8.08, 5.88 Hz), 4.98 (m), 5.15 (m), 5.23 (m), 5.27 (m), 5.7 (d, J = 0.73 Hz), 5.75 (br s), 6.53 (br d, J = 5.88 Hz), 7.05−7.4 (m), 7.47 (d, J = 7.35 Hz), 7.93 (br m), 8.0 (d, J = 9.55 Hz), 8.8 (d, J = 9.55 Hz), 8.9 (d, J = 8.08 Hz); exact mass calcd for $C_{59}H_{91}N_8O_{11}$ 1087.6807, found 1087.6835. The second eluate gave **7B** (31.5 mg, 6.6%): Analytical HPLC retention time, 9.82 min; IR (KBr) ν 3322, 2964, 2876, 1750, 1637 cm^{-1}; ^{1}H NMR (500 MHz) δ 0.60−1.15 (m), 1.18 (br m), 1.25 (s), 1.3 (s), 1.33 (s), 1.35−1.70 (m), 1.73−1.85 (m), 1.85−2.20 (br m), 2.30 (br m), 2.47 (s), 2.53 (br m), 2.65 (m), 2.70 (s), 2.80 (s), 2.9 (s), 2.95 (m), 3.05 (br s), 3.07 (m), 3.10 (s), 3.13 (m), 3.18 (s), 3.23 (m), 3.28 (s), 3.35 (s), 3.55 (m), 3.65 (m), 3.75 (m), 3.83 (d, J = 3.83 Hz), 4.2 (br t, J = 7.35, 7.35 Hz), 4.53 (br d, J = 11.02 Hz), 4.60 (m), 4.65 (m), 4.75 (m), 4.88 (m), 4.9 (m), 5.0 (m), 5.17 (m), 5.33 (m), 5.57 (br s), 5.63 (br s), 6.55 (br s), 7.0 (br d, 7.35 Hz), 7.05−7.4 (m), 7.93 (br d, J = 3.67), 8.0 (br s), 8.8 (m); exact mass calcd for $C_{59}H_{91}N_8O_{11}$ 1087.6807, found 1087.6835. The third eluate gave **7C** (45.3 mg, 8.7%): Analytical HPLC retention time, 10.55 min; IR (KBr) ν 3322, 2964, 2877, 1742, 1633 cm^{-1}; ^{1}H NMR (500 MHz) δ 0.65 (m), 1.23 (br d, J = 7.35 Hz), 1.35 (d, J =7.35 Hz), 1.40 (d, J = 7.35 Hz), 1.50 (m), 1.6 (m), 1.7 (m), 1.78 (m), 1.9 (m), 2.05 (m), 2.13 (m), 2.0 (br s), 2.28 (m), 2.43 (br s), 2.50 (s), 2.65 (m), 2.75 (s), 2.80 (m), 2.95 (s), 3.03 (s), 3.05 (m), 3.10 (s), 3.12 (m), 3.15 (s), 3.17 (s), 3.19 (s), 3.22 (m), 3.28 (br s), 3.58 (m), 3.63 (br d, J = 13.23 Hz), 3.75 (m), 3.85 (br d, J = 8.82 Hz), 4.2 (m), 4.4 (m), 4.5 ((t, 8.08, 8.08 Hz), 5.53 (t, 11.0, 11.0 Hz), 4.63 (m), 4.75 (m), 4.85 (m), 4.9 (m), 5.0 (m), 5.15 (m), 5.3 (m), 5.55 (br s), 5.65 (br s), 6.55 (br d, J 5.88 Hz), 7.05−7.35 (m), 7.4 (m), 7.95 (br d, 7.35 Hz), 8.1 (m), 8.8 (br d, J = 7.35 Hz); exact mass calcd for $C_{59}H_{91}N_8O_{11}$ 1087.6807, found 1087.6840. The fourth eluate gave **7D** (104.7 mg, 20.1%): Analytical HPLC retention time, 11.49 min; IR (KBr) ν 3324, 2964, 2876, 1747, 1633 cm^{-1}; ^{1}H NMR (500 MHz) δ 0.65−1.1 (m), 1.15 (m), 1.23 (s), 1.24−1.60 (m), 1.65 (m), 1.66−1.95 (m), 2.05 (m), 2.15 (br s), 2.28 (m), 2.43 (br m), 2.47 (s), 2.65 (s), 2.9 (m), 3.05 (s), 3.10 (m), 3.13 (s), 3.15 (s), 3.23 (m), 3.29 (s), 3.27 (s), 3.32 (s), 3.55 (m), 3.63 (dd, J = 14.7, 5.88 Hz), 3.75 (m), 3.8 (br s), 3.87 (br s), 4.18 (t, J = 9.56 Hz), 4.44 (dd, J = 11.03, 5.88 Hz), 4.61 (d, J = 11.03 Hz), 4.83−4.98 (m), 4.99 (d, J = 11.03 Hz), 5.16 (d, J = 11.03 Hz), 5.21 (m), 5.27 (d, J = 11.76 Hz), 5.74 (d, J = 2.21 Hz), 5.76 (d, J = 1.47 Hz), 6.49 (d, J = 6.62 Hz), 7.05−7.40 (m), 7.51 (d, J = 7.35 Hz), 7.35 (d, J = 8.58 Hz), 7.93 (d, J = 8.08 Hz), 7.95 (d, J = 7.35 Hz), 8.84 (d, J = 9.56 Hz), 8.86 (d, J = 9.56 Hz); exact mass calcd for $C_{59}H_{91}N_8O_{11}$ 1087.6807, found 1087.6819.

8-(3-Hydroxy-*N*-methylnorleucine)aureobasidin A (8).

According to a procedure similar to that described for **3**, to R106-sarcosine (0.5 g, 0.48 mmol), and LiCl (161 mg, 3.8 mmol) in dry THF (5 mL) was added 0.35 M LDA (6.8 mL) followed by 1.6 M *n*-butyllithium (1.45 mL) and butyraldehyde (0.69 mL, 7.6 mmol). The residue was purified by C-18 reversed phase chromatography (38:62 water/acetonitrile, Waters 3x 40 × 10 Nova-Pak radial cartridges, 75 mL/min, 250 nm). The first eluate gave **8A** (56.6 mg, 10.6%): Analytical HPLC retention time, 16.95 min; IR (KBr) ν 3332, 2964, 2876, 1748, 1636 cm^{-1}; ^{1}H NMR (500 MHz) δ 0.53 (d, J = 3.89 Hz), 0.54−1.05 (m), 1.06 (d, J = 7.79 Hz), 1.14 (d, J = 8.59 Hz), 1.25 (s), 1.94−1.26 (m), 2.06 (m), 2.27 (m), 2.48 (d, J = 5.88 Hz), 2.55 (s), 2.60 (s) 2.70 (m), 2.71 (s), 2.74 (s), 2.82 (s), 2.88 (d, J = 13.23 Hz), 2.94−3.01 (m), 3.02 (s), 3.04 (s), 3.06 (s), 3.07−3.13 (m), 3.15 (m), 3.18−3.27 (m), 3.28 (s), 3.29 (s), 3.31 (s), 3.33 (s), 3.46 (d, J = 5.88 Hz), 3.54 (m), 3.65 (dd, J = 16.17, 3.67 Hz), 3.74 (d, J = 9.55 Hz), 4.0 (m), 4.13 (m), 4.19 (t, J = 9.55, 9.55 Hz), 4.34 (d, J = 5.64 Hz), 4.46 (m), 4.51 (d, J = 0.6 Hz), 4.55 (d, J = 10.29 Hz), 4.58 (d, J = 7.35 Hz), 4.83 (dd, J = 9.55, 5.51 Hz), 4.9 (m), 4.97 (d, J = 11.02 Hz), 5.05−5.21 (m), 5.22 (d, J = 11.02 Hz), 5.74 (m), 5.28 (s), 5.30 d, J = 7.35 Hz), 5.52 (t, 5.88, 5.88 Hz), 5.7 (m), 5.74 (d, J = 1.83 Hz), 5.77 (d, J = 1.47 Hz), 6.54 (d, J = 7.35 Hz), 6.68 (m), 6.99−7.40 (m), 7.51 (d, J = 7.35 Hz), 7.86 (m), 7.95 (d, J = 7.93 Hz), 7.96 (d, J = 10.29 Hz), 8.83 (d, J = 11.02 Hz), 8.88 (d, J = 8.08 Hz); exact mass calcd for $C_{61}H_{95}N_8O_{11}$ 1115.7120, found 1115.7154. The second eluate gave **8B** (1.0 mg, 0.19%): Analytical HPLC retention time, 17.99 min; IR (KBr) ν 3324, 2964, 2876, 1742, 1633 cm^{-1}; ^{1}H NMR (500 MHz) δ 0.58 (m), 0.65−1.13 (m), 1.16 (d, J = 9.18 Hz), 1.23 (s), 1.24−1.62 (m), 1.66−1.93 (m), 1.95−2.12 (m), 2.27 (m), 2.45 (m), 2.47 (s), 2.65 (s), 2.88 (d, J = 12.86 Hz), 2.91 (d, J = 12.86 Hz), 3.04 (s), 3.09 (m), 3.15 (s), 3.15 (s), 3.25 (m), 3.27 (s), 3.29 (s), 3.31 (s), 3.53 (m), 3.63 (dd, J = 16.17, 3.68 Hz), 3.74 (m), 3.83 (br s), 4.17 (t, J =9.18, 9.18 Hz), 4.42 (dd, 8.82, 5.88 Hz), 4.53 (d, J = 8.82 Hz), 4.56 (d, J = 8.82 Hz), 4.77 (d, J = 7.35 Hz), 4.85 (m), 4.90 (m), 4.98 (dd, J = 7.35, 5.51 Hz), 5.0 (d, J = 9.18 Hz), 5.15 (d, J = 11.02 Hz), 5.23 (m), 5.26 (d, J = 9.18 Hz), 5.28 (s), 5.74 (d, J = 1.1 Hz), 5.76 (d, J = 1.1 Hz), 6.50 (d, J = 7.35 Hz), 7.05−7.40 (m), 7.52 (d, J = 7.35 Hz), 7.87 (d, J = 7.35 Hz), 7.92 (d, J = 9.18 Hz), 8.82 (d, J = 11.02 Hz), 8.86 (d, J = 9.18 Hz); exact mass calcd for $C_{61}H_{95}N_8O_{11}$ 1115.7120, found 1115.7144. The third eluate gave **8C** (19.9 mg, 3.7%): Analytical HPLC retention time, 18.93 min; IR (KBr) ν 3322, 2964, 2876, 1744, 1633 cm^{-1}; ^{1}H NMR (500 MHz) δ 0.60−1.15 (m), 1.17 (d, J = 8.08 Hz), 1.25 (s), 1.32−1.95 (m), 2.28 (m), 2.48 (m), 2.50 (s), 2.54 (s), 2.73 (m), 2.88−2.98 (m), 3.02 (s), 3.08−3.12 (m), 3.13 (s), 3.15 (s), 3.18 (br d, J = 3.67 Hz), 3.19 (s), 3.25−3.29 (m), 3.30 (s), 3.33 (m), 3.56 (m), 3.66 (dd, J = 14.7, 5.51 Hz), 3.75 (br q, J = 11.05, 11.05 Hz), 3.81 (d, J = 9.18 Hz), 4.04 (m), 4.12 (m), 4.21 (br t, J = 9.18, 9.18 Hz), 4.32 (m), 4.54 (m), 4.78 (d, J = 7.35 Hz), 4.81−5.87 (m), 5.10 (d, J = 5.88 Hz), 5.18 (m), 55.24−5.28 (m), 5.29 (s), 5.30−5.39 (m), 5.62 (d, J = 1.83 Hz), 5.66 (d, J = 1.83 Hz), 6.56 (d, J = 6.61 Hz), 7.04−7.24 (m), 7.25 (s), 7.26−7.35 (m), 7.37 (d, J = 6.61 Hz), 7.90 (d, J = 8.82 Hz), 7.95 (d, J = 7.95 Hz), 8.80 (d, J = 8.85 Hz), 8.88 (d, J = 7.35 Hz); exact mass calcd for $C_{61}H_{95}N_8O_{11}$ 1115.7120, found 1115.7154. The fourth eluate gave **8D** (91.8 mg, 17.2%): Analytical HPLC retention time, 22.66 min; IR (KBr) ν 3322, 2964, 2875, 1733, 1633 cm^{-1}; ^{1}H NMR (500 MHz) δ 0.60−1.15 (m), 1.17 (d, J = 7.35 Hz), 1.25 (s), 1.30 (m), 1.35−1.70 (m), 1.75 (br s), 1.80 (m), 1.90 (m), 2.05 (m), 2.30 (m), 2.45 (s), 2.50 (br s), 2.57 (s), 2.77 (s), 2.90−2.97 (m), 3.0 (s), 3.05−3.15 (m), 3.16 (s), 3.18 (m), 3.2 (s), 3.25 (s), 3.30 (br d, J = 3.685 Hz), 3.33 (s), 3.55 (m), 3.65 (m), 3.75 (m), 3.80 (d, J = 8.82 Hz), 4.2 (br t, J = 7.35, 7.35 Hz), 4.4 (m), 4.5 (m), 4.75 (br d, J = 7.35 Hz), 4.90 (m), 5.0 (m), 5.20 (m), 5.33 (m), 5.64 (d, J = 1.0 Hz), 5.66 (d, J = 1 Hz), 6.57 (d, J = 5.88 Hz), 7.0 (d, J = 7.35 Hz), 7.05−7.40 (m), 7.9 (d, J = 11.02 Hz), 7.95 (d, J = 8.82 Hz), 8.77 (d, J = 8.82 Hz), 8.83 (d, J = 11.02 Hz); exact mass calcd for $C_{61}H_{95}N_8O_{11}$ 1115.7120, found 1115.7144.

Computational Method. In order to understand the origin of the thermodynamic stability of R106-1, **1**, we carried out a computational study of several isomers of this molecule. The X-ray crystal structure[4] of R106-1 was used as a starting geometry for all isomers. Three structures of each isomer were generated by simple rotation of the 2-propanol side chain of residue β OH Me-Val-8 to the three staggered orientations. Each of the six structures were fully optimized with the AM1 semiempirical method[13] using the MOPAC 6.02 program[17] on a CRAY-2/128S supercomputer. The calculations also explore the use of the option to use a molecular mechanics correction to insure planarity of amide linkages. As shown in Tables 3 and 4 use of this option only changes the results slightly. All structures were optimized to a root mean square gradient norm less than 0.01. All stationary points were characterized as local minima on the potential surface by a force calculation. In this all-atom representation of R106-1 there are 171 atoms which makes even simple energy minimization on a supercomputer resource intensive. (All the calculations performed in this study took approximately 600 h of cpu time.) The procedure for determining the thermodynamic stabilities of the isomers of **7** was done in a similar fashion as for R106-1.

The X-ray crystal structure[4] of R106-1 was fully optimized with the AM1 method.[13] The rms difference of the fully optimized AM1 structure of isomer **1-L-a** and the X-ray crystal structure of R106-1 is 0.32 Å for the 27 cyclic backbone atoms and 0.62 Å for all 79 non-hydrogen atoms. These low values of rms difference for the AM1 structure indicates that there is little deviation of geometry from that of the X-ray crystal structure.

Calculations to understand the origins of the alkylation selectivities were performed by starting from the fully optimized minima and assuming a CA$\cdots$ CB bond length of 2.20 Å and a CA-CB-OG tetrahedral attack angle of 109°.[18] In these model calculations only the residue 8 side chain was optimized. All attempts to optimize all variables besides the attack angle and distance failed to optimize to completion within 50 h of cpu time on our CRAY computer. Thus, this simpler model for alkylation selectivity was used to investigate the differences in energetics for structures leading to the D and L isomers.

Supporting Information Available: Experimental procedure, HRMS data, C18 HPLC analytical analysis, and 300 MHz ^{1}H NMR spectra of 8-(4,4,4-trifluoro-*N*,3-dimethylthreonine)aureobasidin A, 500 MHz ^{1}H NMR spectra for **3**−**8**, and a summary table of ^{1}H NMR chemical shifts of Cγ(Ar)-*H*, MePhe and 2-C*H*, HMP for **3**−**6** (21 pages). This material is contained in libraries on microfiche, immediately follows this article in the microfilm version of the journal, and can be ordered from the ACS; see any current masthead page for ordering information.

JO951485Q

(17) Stewart, J. J. P. MOPAC, Ver. 6.02, QCPE No. 455, Indiana University, Bloomington, IN, as modified for the Silicon Graphics workstation.

(18) (a) Houk, K. N.; Li, Y.; Evanseck, J. D. *Angew. Chem., Int. Ed. Engl.* **1992**, *31*, 682. (b) Houk, K. N.; Paddon-Row, M. N.; Rondan, N. G.; Wu, Y.-D.; Brown, F. K.; Spellmeyer, D. C.; Metz, J. T.; Li, Y.; Loncharich, R. J. *Science* (*Washington, DC*) **1986**, *231*, 1108.